

Pediatric Chest MR Imaging: Lung and Airways



Juan C. Baez, MD^{a,b}, Pierluigi Ciet, MD, PhD^{c,d}, Robert Mulkern, PhD^b, Ravi T. Seethamraju, PhD^e, Edward Y. Lee, MD, MPH^{b,*}

KEYWORDS

• MR imaging • Lungs • Airways • Pediatric patients

KEY POINTS

- Magnetic resonance (MR) imaging can reliably identify lung nodules larger than 5 mm in children.
- MR imaging can permit accurate and dynamic evaluation of large airways.
- MR imaging is a valuable imaging modality to assess the progression of chronic lung diseases such as cystic fibrosis.
- Future chest MR imaging techniques have a great promise for functional imaging of the lungs in pediatric patients.

INTRODUCTION

In recent years, MR imaging with advanced imaging techniques has been receiving a lot of attention mainly because of its ability to assess lungs and airways in the pediatric population. Although computed tomography (CT), which is regarded as the gold standard imaging modality, provides exquisite resolution of the anatomic structures of the lungs and airways, it exposes the pediatric patient to ionizing radiation. MR imaging has been advocated as an adjunctive tool, particularly in pediatric patients, for the evaluation of chest pathology. In the past, the proton-poor environment, rapid signal dephasing, and respiratory motion presented significant obstacles for widespread adoption and clinical use of MR imaging lung studies. Nevertheless, by optimizing protocols and tailoring them to the individual pediatric

patient and with the clinical question at hand, MR imaging can now provide excellent visualization of the relevant anatomy and pertinent abnormalities. The future of chest MR imaging includes a greater emphasis on functional information. The use of hyperpolarized gases, where available, provides excellent imaging of lung ventilation. Upcoming technologies, such as Fourier decomposition, promise the ability to provide functional perfusion and ventilation data without the use of intravenous or inhaled contrast agents. The overarching goal of this article is to provide up-to-date information regarding MR imaging techniques for practical assessment of lungs and airways in the pediatric population. Furthermore, several pediatric thoracic disorders involving the lungs and airways that can be evaluated with advanced MR imaging techniques are highlighted.

Disclosures: no relevant disclosures (J.C. Baez, P. Ciet, R. Mulkern, and E.Y. Lee); Dr Seethamraju has stock ownership and an employment affiliation with Siemens AG.

^a Mid-Atlantic Permanente Medical Group, 2101 East Jefferson Street, Rockville, MD 20852, USA;

^b Department of Radiology, Boston Children's Hospital, Harvard Medical School, 300 Longwood Avenue, Boston, MA 02115, USA; ^c Department of Radiology and Pediatric Pulmonology, Sophia Children's Hospital, Erasmus Medical Center, Wytemaweg 80, 3015 CN, Rotterdam, The Netherlands; ^d Department of Radiology, Beth Israel Deaconess Medical Center, Harvard Medical School, 330 Brookline Ave, Boston, MA 02215, USA;

^e Magnetic Resonance, Research and Development, Siemens Healthcare, 1620 Tremont St., Boston, MA 02120, USA

* Corresponding author. Department of Radiology, Boston Children's Hospital, Harvard Medical School, 300 Longwood Avenue, Boston, MA 02115.

E-mail address: Edward.Lee@childrens.harvard.edu

Magn Reson Imaging Clin N Am 23 (2015) 337–349

<http://dx.doi.org/10.1016/j.mric.2015.01.011>

1064-9689/15/\$ – see front matter © 2015 Elsevier Inc. All rights reserved.

EVALUATION OF LUNG PARENCHYMAL ABNORMALITIES

MR Imaging Protocol

A fundamental MR imaging protocol evaluating the lung parenchyma includes a gradient recalled echo (GRE) multiplanar localizer, coronal T2 single-shot half Fourier turbo spin echo (HASTE), axial 3-dimensional (3D) GRE T1, coronal balanced steady-state free precession (true fast imaging with steady-state precession), and axial short tau inversion recovery.^{1,2} One can complete this practical MR imaging examination in less than 25 minutes. If necessary, postcontrast imaging with a 3D GRE T1-weighted sequence with fat saturation can provide information regarding enhancement characteristics. Pediatric patients with difficulty after breathing instructions because of their young age or critical condition often benefit from a sequence that does not rely on breath holds such as an axial T2 periodically rotated overlapping parallel lines with enhanced reconstruction (PROPELLER/BLADE) performed with the patient free breathing.

Consolidation and Infection

Although CT remains the gold standard for evaluation of parenchymal lung abnormalities, the ability to characterize lung abnormality without exposing the child to ionizing radiation has propelled research into the use of alternative technology.³ Several studies have shown that ultrasonography can diagnose peripherally located lung consolidation as well as or better than radiography.⁴⁻⁶ However, chest ultrasonography becomes more difficult with increasing age because the acoustic windows become more limited with increasing ossification of the skeletal structures.⁷

Furthermore, deep parenchymal abnormalities surrounded by aerated lung go undetected by ultrasonography because of dissipation of the ultrasound beam by the air interface. For these reasons, the use of MR imaging to aid in the diagnosis of lung abnormalities has been evaluated by multiple investigators.^{8,9} Although CT provides greater spatial resolution than MR imaging, the use of multiple sequences offers characterization of tissue beyond the limits of CT.¹⁰

Studies have shown that MR imaging can detect pneumonia and other consolidative processes in the lungs (**Figs. 1** and **2**). A prospective study comparing 1.5T MR imaging using fast T1 and T2 imaging sequences with radiography for the detection of pneumonia proved that the 2 modalities were comparable.¹¹ A comparison of different MR pulse sequences showed that HASTE was the best sequence for the detection of lung consolidation.² In addition to the consolidation, MR imaging can also detect complications of pneumonia such as necrosis/abscess and pneumonia.

Other studies have compared MR imaging with CT, the current gold standard, and shown that the former is a high-sensitivity examination for evaluation of lung abnormalities. In one recent prospective trial of 71 pediatric patients in which patients underwent both CT and MR imaging evaluation within 24 hours, diagnostic accuracy of MR imaging was 97% compared with that of CT. The only undiagnosed lung findings were a single case of mild bronchiectasis and another case with a pulmonary nodule measuring 3 mm that went undetected.¹² In addition, this study demonstrated excellent interobserver reliability between 2 readers, suggesting the robustness of this technique.

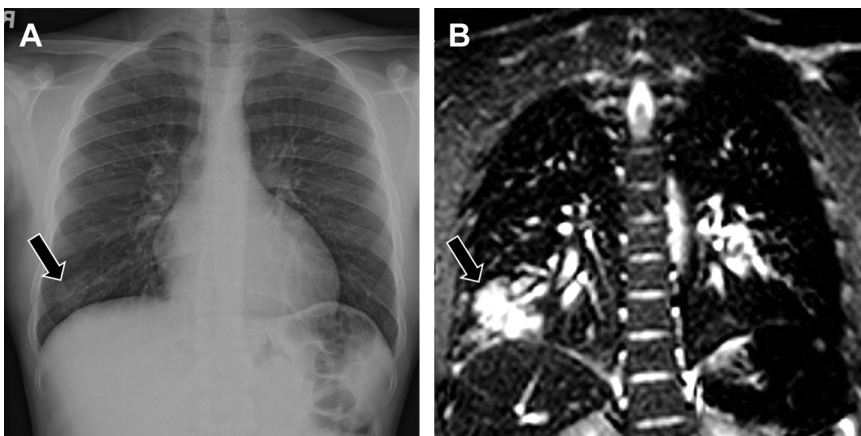


Fig. 1. Pneumonia. (A) Frontal chest radiograph demonstrates focal consolidative opacity (*arrow*) in the right lung base. (B) Coronal short tau inversion recovery MR image demonstrates a T2-hyperintense focus (*arrow*) in the right lower lobe corresponding to the consolidative opacity (see Fig. 1A) in this region.

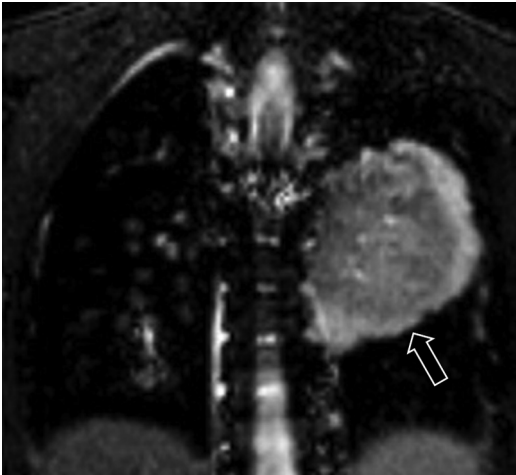


Fig. 2. Round pneumonia in an 8-year-old girl who presented with fever and cough. Coronal short tau inversion recovery MR image demonstrates a round consolidative opacity (*arrow*). Follow-up chest radiograph obtained after treatment demonstrated interval resolution.

Although MR imaging is unlikely to define the causative agent in infection, clues gleaned from the imaging may help narrow the differential diagnosis in cases in which additional imaging is performed for problem solving. Lung necrosis in tuberculosis, for example, can appear low in signal intensity on fluid-sensitive sequences likely because of the underlying caseating necrosis associated with *Mycobacterium*.¹³ Iron deposition within foci of *Aspergillus* infection has also been associated with low signal on MR imaging.¹⁴ Certain infections such as those caused by *Echinococcus* result in a characteristic appearance.

The resultant hydatid cysts present as cystic masses, often with smaller daughter cysts.¹⁵ A T2-hypointense rim has been described in these cystic masses and should at least raise the possibility of this diagnosis (**Fig. 3**).¹⁶

Lung Masses

Congenital lung masses constitute a group of developmental disorders affecting lung parenchyma in vascular and airway development.¹⁷ The diagnosis of congenital lung masses including sequestrations and congenital pulmonary airway malformations (CPAMs) is increasingly being made prenatally with the use of fetal ultrasonography as a screening tool.¹⁸ Also, fetal MR imaging can provide additional information in the evaluation of these abnormalities. In the neonatal period, thoracic MR imaging further aids in characterization of these masses and confirms prenatal diagnoses.^{19,20} The use of T2-weighted sequences often permits reliable differentiation between normal and abnormal lung masses. In addition, T2-weighted imaging can help in identifying cystic components within these masses.²¹ However, large air-filled cysts may go unrecognized on MR imaging because of the lack of signal.

MR imaging may also identify feeding vessels and draining veins associated with congenital lung malformation such as pulmonary sequestration.²² Although one can identify flow voids on multiple MR sequences, MR angiography with postprocessed 3D images best illustrates feeding vessels, as in the case of a pulmonary sequestration wherein the anomalous arterial vessels arise from the aorta.²³ Recent research has suggested that bronchial atresia lies on the same spectrum

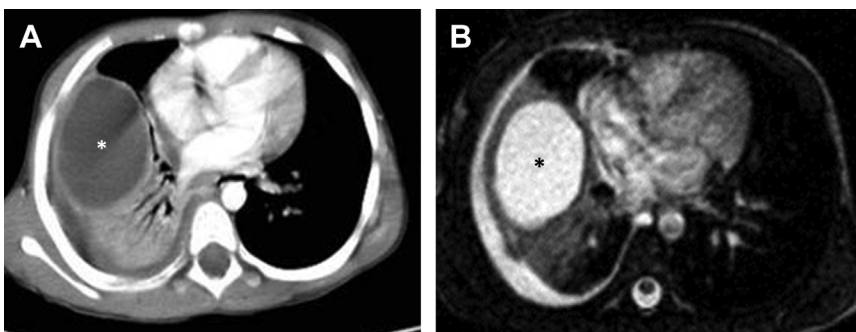


Fig. 3. (A) Hydatid cyst in a 15-year-old boy with known pulmonary hydatid infection who presented with fever, elevated white blood cell count, and opacity in the right lower lung on chest radiographs. Axial contrast-enhanced CT image shows large cystic lesion (*asterisk*) in the right lower lobe consistent with pulmonary hydatid infection. (B) Axial T2-weighted MR image shows large cystic lesion (*asterisk*) in the right lower lobe corresponding to the finding in Fig. 3A. (From Gorkem SB, Coskun A, Yikilmaz A, et al. Evaluation of pediatric thoracic disorders: comparison of unenhanced fast-imaging sequence 1.5T MRI and contrast enhanced MRI. *AJR Am J Roentgenol* 2013;200:1354; with permission.)

as these other types of congenital lung masses.^{24,25} The atretic bronchus is a mucous-filled tubular structure, which is both T1 and T2 hyperintense. Other signs of bronchial atresia such as subtle air trapping, however, likely go unnoticed on MR imaging using standard protocols. The improved spatial resolution of CT compared with that of MR imaging and the ability to visualize air-filled structures and associated complications such as trapped air are a large part of the reason that CT remains the preferred modality for imaging diagnosis and surgical planning.²⁶ Nevertheless, the use of a proton-density-weighted GRE sequence with short repetition time (TR) and echo time (TE) and slice thickness between 5 to 8 mm can often allow detection of trapped air.

Primary lung neoplasms occur far less frequently in the pediatric population than in adults and are less common than metastatic disease.^{27,28} A list of relatively rare diagnoses in this category includes entities such as papillomas, myofibromas, hemangiomas, and hamartomas. Mesenchymal hamartomas are masses that arise from the chest wall, but on presentation may seem as if they arise from the lung (**Fig. 4**). These masses constitute no risk of metastatic or recurrent disease and therefore require no treatment unless symptomatic.²⁹ Characteristic MR imaging features of the mesenchymal hamartomas include hemorrhagic fluid levels within secondary aneurysmal bone cysts and calcification seen as hypointense signal on MR imaging.

Pathologists often classify inflammatory myofibroblastic tumors as benign pulmonary neoplasms, although these lesions sometimes recur or act aggressively.²⁹ These masses often

constitute a diagnostic and clinical dilemma because of their behavior. The other name for this lesion, inflammatory pseudotumor, also indicates that not all pathologists are convinced that these masses are neoplastic. MR imaging features of inflammatory myofibroblastic tumors include low signal on T1, high signal on T2, and homogeneous enhancement (**Fig. 5**).³⁰

Malignant primary lung neoplasms also present in a variety of forms. Pleuropulmonary blastomas are uncommon malignancies with both mesenchymal and epithelial components that can present like CPAMs.^{31,32} Numerous other pediatric primary lung malignancies can, although rarely, arise de novo, with a full discussion of these cancers lying beyond the scope of this article (**Figs. 6 and 7**).

Metastatic Pulmonary Nodules

Use of MR imaging for the detection of pulmonary nodules remains an alluring goal because many pediatric patients with cancer require routine surveillance for detection of lung recurrence or metastases. In these pediatric patients, the cumulative radiation dose of chest imaging may prove significant.^{33,34} Furthermore, these patients may possess increased sensitivity to the damaging effects of radiation with predisposition to developing new malignancies because of prior therapy or congenital sensitivity, such as in pediatric patients with ataxia telangiectasia. Consequently, replacement of routine surveillance CT scans with MR imaging would allow continued evaluation without exposing the child to additional risks.

MR imaging can reliably detect lung nodules larger than 5 mm (**Fig. 8**).¹² Other studies suggest that MR imaging becomes less sensitive for

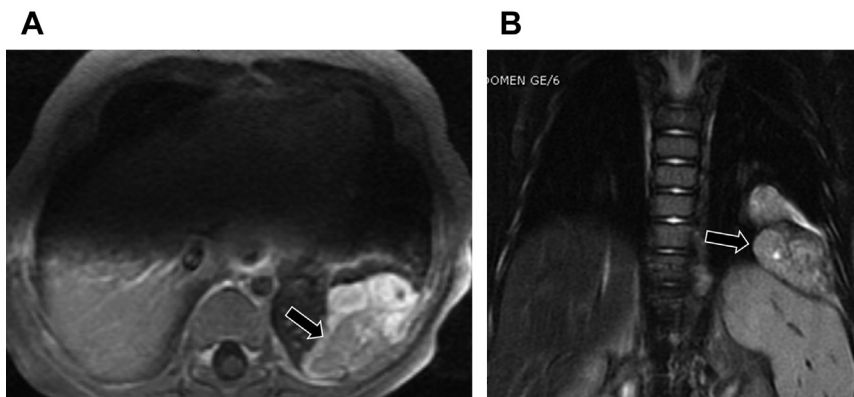


Fig. 4. Mesenchymal hamartoma. (A) Axial T1 postcontrast MR imaging demonstrates heterogeneous enhancement within this well-defined left lower chest wall mass (*arrow*) that proved a mesenchymal hamartoma on surgical excision. (B) Coronal T2-weighted MR image shows a left lower lobe heterogeneous mass (*arrow*) with internal foci of T2 prolongation and areas of susceptibility corresponding to known calcifications.

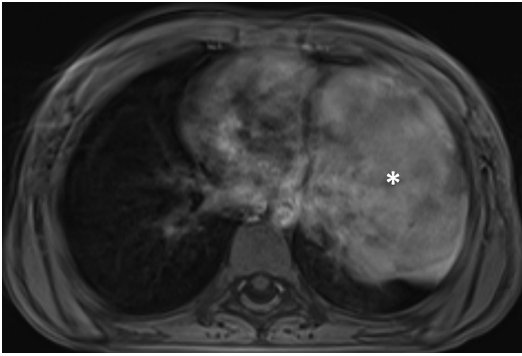


Fig. 5. Myofibroblastic tumor. Axial T1 postcontrast MR image shows homogeneous enhancement in the large lingular mass (*asterisk*).

detection of lung nodules smaller than 3 mm (sensitivity of 73%) (**Fig. 9**).³⁵ A known limitation in MR imaging evaluation concerns calcified lung nodules. Calcification results in susceptibility-related loss of MR imaging signal intensity. Consequently, calcified nodules, which would be easily identified on CT, become occult on MR imaging. The improved tissue contrast, however, may add additional information regarding the cause of the nodule not evident on other imaging. The use of diffusion-weighted MR imaging has been suggested to also aid in both detection and characterization of malignant nodules.^{36,37}

Interstitial Lung Disease

The use of MR imaging for the evaluation of interstitial lung disease remains in an early stage of development. Few studies have compared it to the current radiological gold standard, high-resolution CT.^{38–40} Nevertheless, T2-hyperintense areas that do not obscure the vascular markings correspond to ground glass opacity seen on CT.⁴¹ Curvilinear bands and parenchymal

distortion can also be visualized with MR imaging. The strength of MR imaging for interstitial lung disease, however, potentially resides in exploiting different signal characteristics of tissue to distinguish between active inflammation and fibrosis with inflamed tissue appearing T2 hyperintense. Rapid enhancement kinetics also seems to favor active inflammation.⁴² Additional studies are necessary before MR imaging can play a pivotal role in evaluating interstitial lung disease.³⁹

EVALUATION OF AIRWAYS

Appropriate evaluation of the airway depends on an assessment of the level of the problem. Either the large airways or the small airways can be involved, each with their own pathologic conditions and each requiring different approaches.

Small airways disease is radiologically defined by direct signs, such as bronchiectasis, bronchial wall thickening, and mucous plugging, as well as by indirect signs such as trapped air. Bronchiectasis, bronchial wall thickening, and mucous plugging can be assessed by T2-weighted sequences, either in breath hold (HASTE/single-shot fast spin echo) or in free breathing (PROPELLER/BLADE) methods. However, the diagnostic accuracy of these techniques for detecting bronchiectasis and mucous plugging at the periphery of the lung is currently lower compared with that of CT (**Fig. 10**). In fact, the level of the bronchi, bronchial diameter, wall thickness, and signal within the lumen all affect the ability of the radiologist to make the diagnosis.^{43,44} Air trapping assessment with MR imaging is not as reliable as with CT.¹ The increased air content because of air trapping results in low-signal areas barely distinguishable from the surrounding normal lung parenchyma. One can partially improve detection of air trapping by using large voxel sizes and short TR/TE

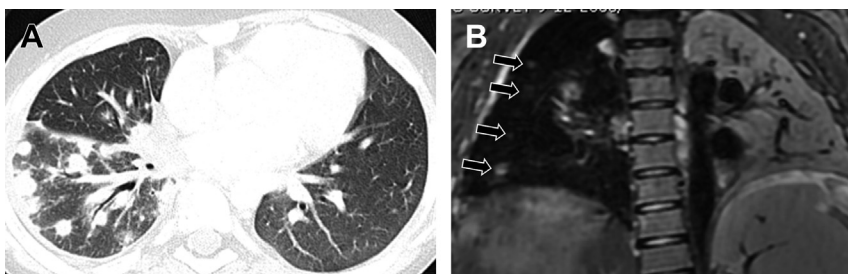


Fig. 6. (A) Pulmonary nodules in a 12-year-old girl with lymphoma. Axial noncontrast chest CT image demonstrates multiple right-sided pulmonary nodules. These pulmonary nodules were proved by biopsy to represent lymphoma. (B) Coronal T2-weighted MR image shows the pulmonary nodules (*arrows*). Extensive atelectasis of the left lung are noted posteriorly.

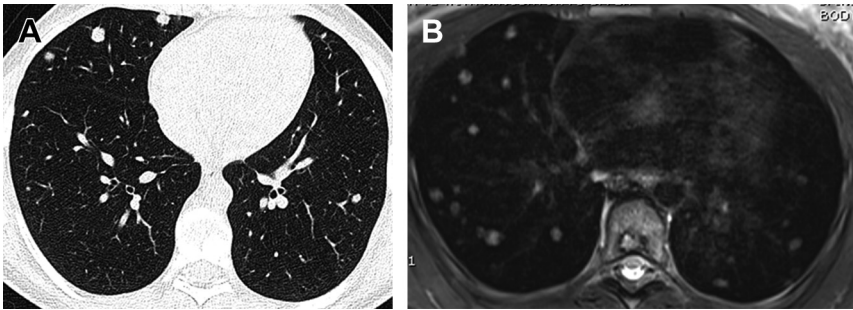


Fig. 7. (A) Epithelioid hemangioendothelioma in a 10-year-old boy. Axial noncontrast CT image demonstrates numerous bilateral pulmonary nodules of varying sizes. (B) Axial T2-weighted MR image of the chest demonstrates numerous bilateral pulmonary nodules correlating with the CT findings (see Fig. 7A).

(**Fig. 11**).⁴⁵ Finally, new techniques such as Fourier decomposition have recently shown promising results for improving the sensitivity of MR imaging for air trapping.⁴⁶

Pathologic condition of the large airway can be subdivided into static and dynamic processes. Most large airway processes fall into the static category with tracheobronchial branching

anomalies, bronchial atresia, tracheal stenosis, neoplasm, and infection residing in this category. MR imaging is well suited for the evaluation of these abnormalities and does not require radically new techniques. The air-filled large airways provide a natural contrast to the surrounding soft tissue because of the paucity of signal (**Fig. 12**). By tracing the black areas representing air in the

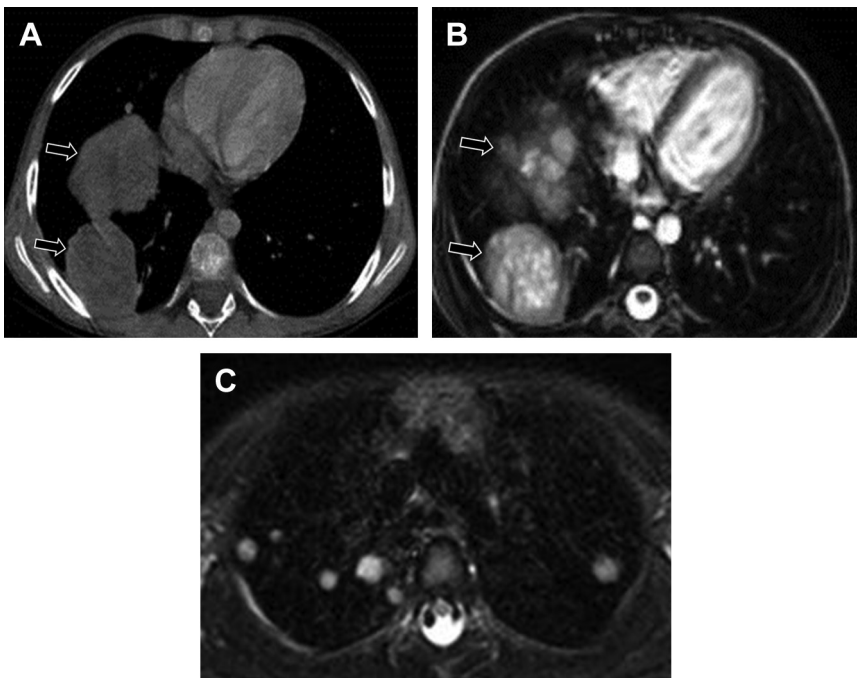


Fig. 8. (A) Metastatic Wilms tumor in a 2-year-old boy. Axial contrast-enhanced CT image demonstrates large masses (*arrows*) in the right lung representing "cannonball" metastases in Wilms tumor. (B) Axial short tau inversion recovery (STIR) MR image again demonstrates the large cannonball metastases (*arrows*) corresponding well with findings seen on CT image (see Fig. 8A). (C) Metastatic Wilms tumor in a 3-year-old girl. Axial STIR MR image shows bilateral smaller pulmonary nodules showing high signal intensity. (From Gorkem SB, Coskun A, Yikilmaz A, et al. Evaluation of pediatric thoracic disorders: comparison of unenhanced fast-imaging sequence 1.5T MRI and contrast enhanced MRI. *AJR Am J Roentgenol* 2013;200:1352-7; with permission.)



Fig. 9. Pulmonary nodule in a 6-year-old boy with Li-Fraumeni syndrome who underwent whole body MR imaging. Coronal T2-weighted MR image of the chest and abdomen demonstrates a 3-mm T2-hyperintense right lower lobe lung nodule (*arrow*).

airway, radiologists can reliably evaluate the airways to the proximal subsegmental branches assuming a high-quality examination without significant artifact.²²

MR Imaging Protocol

Although the previously discussed fundamental lung protocol can also address many airway-

related issues, additional sequences add useful information. A 3D spoiled gradient recalled echo (SPGR) sequence allows evaluation of lung anatomy and measurement of the airway. PD-weighted SPGR helps to depict the tracheal contours that are largely surrounded by mediastinal fat. Dedicated views of the large airways with improved spatial resolution may be obtained by using this sequence on a smaller field of view. Breathing maneuvers can be trained using an MR-imaging-compatible spirometer (**Fig. 13**).⁴⁷ The purpose of the training is to monitor and standardize breathing maneuvers and to reduce anxiety related to the MR imaging investigation, thereby increasing the probability of a successful MR imaging examination. Patients receive adequate training before the examination by a lung function technician who also triggers the image acquisition by closely interacting with the MR imaging technician during the scan.

Tracheobronchomalacia

Dynamic large airway pathology, by definition, changes over time and requires time-resolved imaging for diagnosis. Tracheobronchomalacia is the most common dynamic large airway process and occurs as a result of excessive narrowing or collapse of the airway during the respiratory cycle. Weakness in the airway walls and cartilage results in greater than 50% narrowing of the luminal area during expiration in affected pediatric patients.⁴⁸ Bronchoscopy can directly visualize the airway collapse; however, this is an invasive procedure.^{49,50} Radiography with inspiratory and expiratory views as well as cine fluoroscopy can also attempt to visualize the abnormality; however,

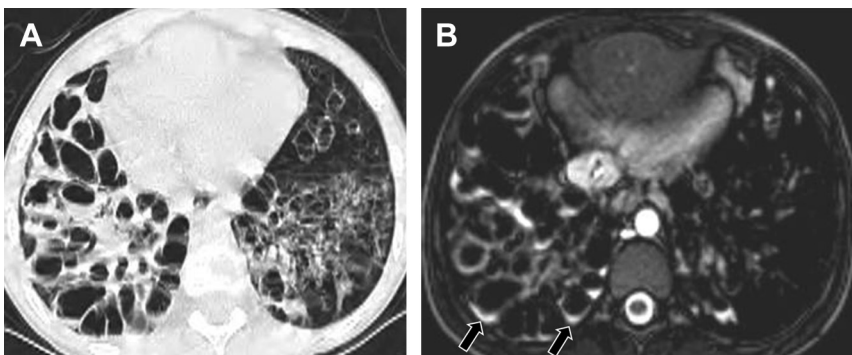


Fig. 10. (A) Cystic bronchiectasis in a 5-year-old girl. Axial CT image demonstrates cystic and cylindrical bronchiectasis, more prominent on the right. Fluid levels are noted in some of the ectatic airways. (B) Axial T2-weighted MR image of the chest demonstrates the same cystic and cylindrical bronchiectasis. The layering fluid (*arrows*) in the airways is again seen and better visualized on MR image. ([A] *Courtesy of Dr Sureyya B. Gorkem, Kayseri, Turkey*; and [B] *From Yikilmaz A, Koc A, Coskun A, et al. Evaluation of pneumonia in children: comparison of MRI with fast imaging sequences at 1.5T with chest radiographs. Acta Radiologica 2011;52(8):914-9; with permission.*)

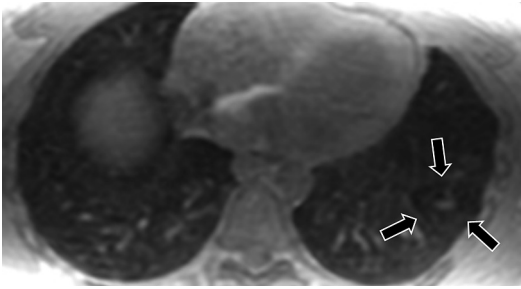


Fig. 11. Air trapping in a pediatric patient with asthma. Axial 3D spoiled gradient echo MR image obtained at expiration using a thick slice, low matrix, and short TR/TE shows air trapping (arrows) in the superior segment of the left lower lobe.

they are limited in sensitivity compared with bronchoscopy.⁵¹ Furthermore, radiography exposes the patient to ionizing radiations. CT, which remains the gold standard of noninvasive imaging of tracheobronchomalacia, allows excellent visualization of the affected anatomy, but it requires at least two phases (inspiratory and expiratory), thus exposing the patient to overall increased radiation.⁵² In addition to exquisite visualization of the airway, CT demonstrates associated pulmonary findings such as air trapping.⁵³ The use of volumetric CT reduces the administered radiation

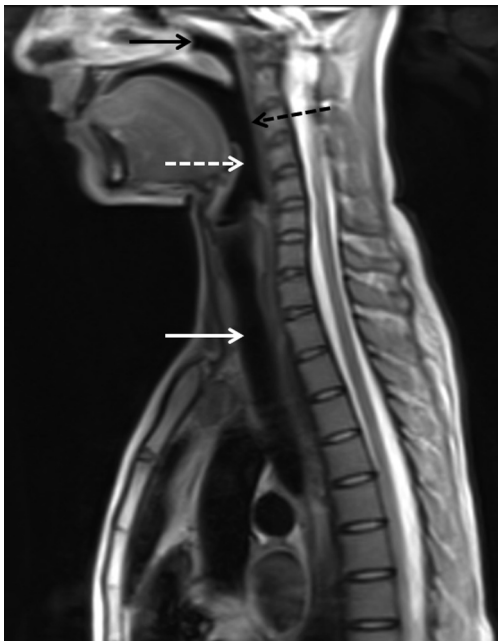


Fig. 12. Airway anatomy in a 5-year-old boy. Sagittal T2-weighted MR image shows the nasopharynx (black solid arrow), oropharynx (black dotted arrow), hypopharynx (white dotted arrow), and trachea (white solid arrow).



Fig. 13. MR-imaging-compatible spirometer. Mouthpiece of an MR-imaging-compatible spirometer is standing on a plastic tripod within the MR imaging suite.

dose while permitting dynamic CT evaluation, but it does not eliminate the radiation exposure.^{54,55}

Spirometer-controlled cine MR imaging provides an alternative noninvasive imaging modality to evaluate for tracheobronchomalacia without exposing the pediatric patient to ionizing radiations.⁴⁷ Four-dimensional time-resolved imaging of the same field of view during specific breathing maneuvers, such as forced expiration, best elicits the collapse point in patients with tracheomalacia (Figs. 14 and 15).

Cystic Fibrosis

Despite the lower spatial resolution of MR imaging compared with that of CT, the improved tissue characterization provided by different MR imaging sequences suggests that it may play an increasingly important role in certain patient populations

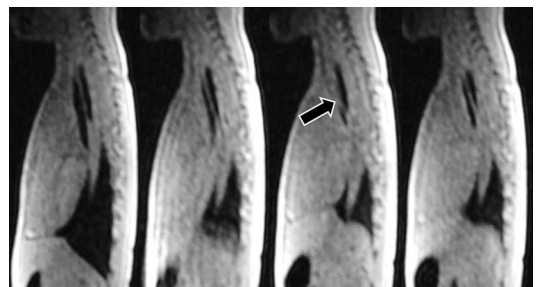


Fig. 14. Tracheomalacia. Time-resolved imaging of contrast kinetics/Time-resolved angiography With Intercalated Stochastic Trajectories (TRICKS/TWIST) in the sagittal plane demonstrates the dynamic appearance of the airway during forced expiration. A total of 48 frames are collected in 22 seconds for a temporal resolution of 500 milliseconds. Trachea completely collapses in the third image (arrow).

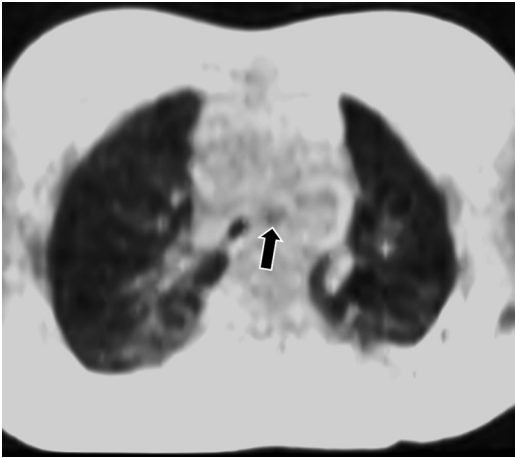


Fig. 15. Bronchomalacia. Axial PD-weighted MR image obtained during forced expiration demonstrates collapse (*arrow*) of the left main stem bronchus. Of note, patent right main stem bronchus is seen at this level.

such as those afflicted with cystic fibrosis.⁵⁶ Patients with cystic fibrosis undergo numerous imaging studies throughout their lives to better assess progression of their disease and determine management. In an effort to quantify disease progression and identify abnormalities before changes in pulmonary function tests, multiple scoring systems have been used, which rely on different imaging modalities including radiography, CT, and now MR imaging. Most of these scoring systems evaluate similar parameters including bronchiectasis, mucous plugging, lung

volumes, and parenchymal changes, with some investigators suggesting that bronchiectasis is the most important parameter.⁵⁷ Recent studies have attempted to validate MR imaging scoring systems by comparing with the CT equivalent and have shown that the results are comparable, suggesting that one may follow-up patients with cystic fibrosis less frequently with ionizing radiation examinations and perform MR imaging instead.⁵⁸

In addition to simply proving comparable to CT, MR imaging can provide additional diagnostic data that are not available from CT. For example, although CT shows bronchial wall thickening well, it cannot characterize the underlying cause. The improved tissue contrast of MR imaging shows T2 hyperintensity within the bronchial wall if it is edematous and shows gadolinium enhancement in cases of active inflammation (**Figs. 16** and **17**).²² The presence of air fluid levels within a dilated bronchus indicates contemporaneous infection. Although parenchymal changes such as consolidation and air bronchograms are seen just as well in MR imaging as in CT, the ability to directly assess lung function is unique to MR imaging. As cystic fibrosis destroys lung parenchyma and impairs ventilation, reflexive vasoconstriction occurs (Euler-Liljestrand reflex). Contrast-enhanced MR perfusion imaging demonstrates perfusion defects that correlate with diseased lung and precede the morphologic changes (**Fig. 18**).⁵⁶

Direct visualization of small airways disease may ultimately be better performed with hyperpolarized

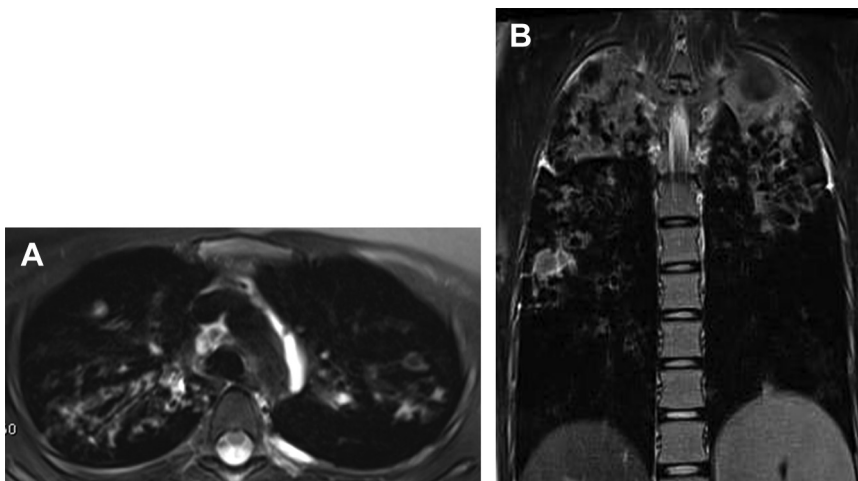


Fig. 16. Cystic fibrosis in a 17-year-old girl. (A) Axial T2-weighted MR image shows bilateral upper lobe bronchiectasis, right lung more severely affected than the left lung. Bronchial wall edema and mucous plugging is best seen in the right upper lobe. (B) Coronal T2-weighted MR image demonstrates bilateral upper-lobe-predominant bronchiectasis, mucous plugging, and consolidative opacities. (Courtesy of Goffredo Serra, MD, Rome, Italy)

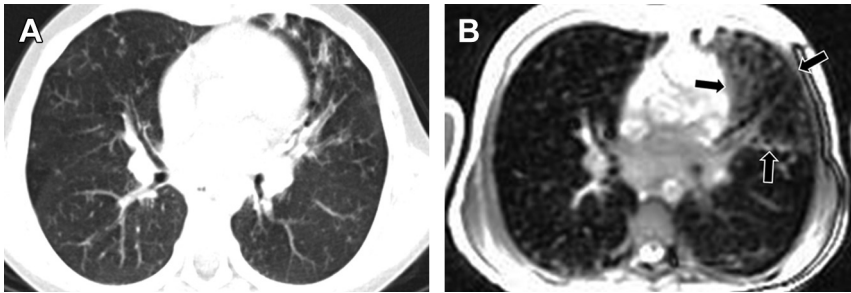


Fig. 17. Cystic fibrosis. (A) Axial noncontrast CT image demonstrates bronchiectasis and bronchial wall thickening, which is most evident in the lingula. (B) Axial T2-weighted MR image redemonstrates the bronchiectasis (arrows). The bronchial walls are thickened and edematous.

gas imaging or oxygen-enhanced imaging, 2 different investigational techniques that may eventually become part of the clinical evaluation of patients with small airways disease.^{22,59}

FUTURE DIRECTIONS

Hyperpolarized gas is a tool currently in the research stage that allows radiologists to overcome the limitations of low ^1H MR imaging signals because of the low proton density in gas-filled lungs. Instead of obtaining MR signal from protons, the MR scanners operate at radiofrequencies sensitive to the resonant frequencies of either ^{129}Xe or ^3He nuclei, gases that are inhaled by the patient immediately preceding the scan. Both hyperpolarized gases (ie, ^{129}Xe and ^3He) produce excellent image quality, although the higher atomic weight of ^{129}Xe could make this agent more sensitive to airflow abnormalities. Furthermore, significant differences in the tissue

permeability of ^3He (impermeable) and ^{129}Xe (very permeable) offer different and possibly complementary information regarding lung structure and function. The safety and efficacy of this technique suggest that it may soon enter into routine clinical practice particularly nowadays with advances in polarizer technology.⁶⁰

Fourier decomposition is a new MR technique that provides perfusion and ventilation images without administration of intravenous or gaseous contrast agents. This technique uses a high-temporal-resolution steady-state free precession sequence to acquire thick slab coronal images in free breathing conditions. The images are first lined up using a nonrigid registration algorithm. Next, by computing voxelwise Fourier decomposition of the time series, the signal originating from the blood perfusion is separated (decomposed) from the signal related to the breathing cycle (Fig. 19). A recent study with Fourier decomposition has proved that this

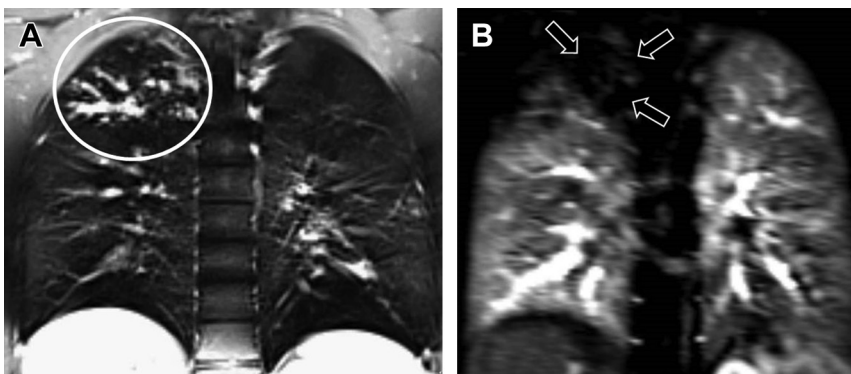


Fig. 18. Cystic fibrosis. (A) Coronal PROPELLER/BLADE proton-density-weighted MR image shows area of bronchiectasis and mucous impaction in the right upper lobe, which results in low parenchyma intensity because of air trapping (white oval). (B) Coronal TRICKS/TWIST, dynamic magnetic resonance angiography (MRA) with k-space manipulation image shows the same area of lung structural changes that is hypoperfused (arrows). (Courtesy of Goffredo Serra, MD, Rome, Italy.)

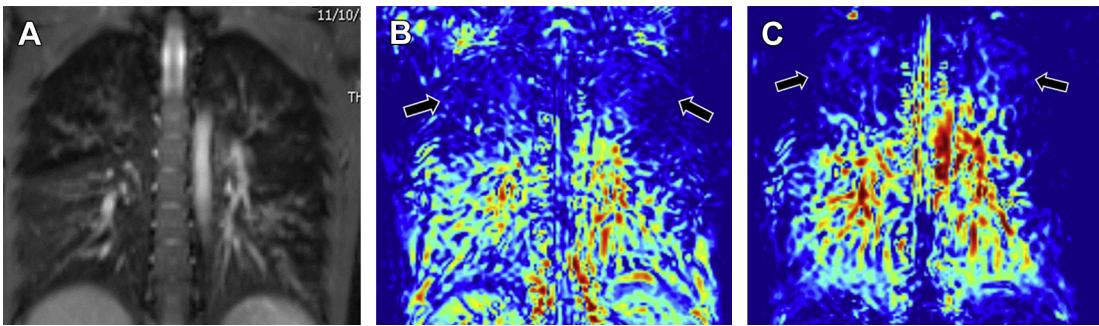


Fig. 19. (A) Air trapping detected in Fourier decomposition MR image. Coronal balanced steady-state free precession/true fast imaging with steady-state precession demonstrates bilateral upper-lobe-predominant bronchial wall thickening and bronchiectasis, which result in air trapping (low signal). (B) Ventilation defect detected in Fourier decomposition MR image. Ventilation map demonstrates decreased ventilation (arrows) in the lung apices compared with the lung bases. (C) Perfusion defect detected in Fourier decomposition MR image. Perfusion map shows that the bilateral lung apices are also hypoperfused (arrows). (Courtesy of Giovanni Morana, MD, PhD, Treviso, Italy.)

technique is feasible in pediatric populations and may represent an elegant alternative to intravenous contrast agents and hyperpolarized gases.⁴⁶

SUMMARY

The performance of high-quality thoracic MR imaging in the pediatric population requires close attention to patient preparation, which includes patient selection, protocol optimization, and appropriate sedation strategies. In addition, it also requires a clear understanding of the basic physics principles as well as the appearance of varied pathologic entities. Although the learning curve may appear steep, the potential rewards of added diagnostic information without the cost of radiation exposure to the child provide excellent motivation to incorporate thoracic MR imaging into daily practice. Current applications have already proved its practical value, and future applications have a great potential to improve its importance and encourage its widespread use.

REFERENCES

- Rajaram S, Swift AJ, Capener D, et al. Lung morphology assessment with balanced steady-state free precession MR imaging compared with CT. *Radiology* 2012;263(2):569–77.
- Fink C, Puderbach M, Biederer J, et al. Lung MRI at 1.5 and 3 Tesla: observer preference study and lesion contrast using five different pulse sequences. *Invest Radiol* 2007;42(6):377–83.
- Liu J. Lung ultrasonography for the diagnosis of neonatal lung disease. *J Matern Fetal Neonatal Med* 2014;27(8):856–61.
- Darge K, Chen A. Point-of-care ultrasound in diagnosing pneumonia in children. *J Pediatr* 2013; 163(1):302–3.
- Reissig A, Copetti R, Mathis G, et al. Lung ultrasound in the diagnosis and follow-up of community-acquired pneumonia: a prospective, multicenter, diagnostic accuracy study. *Chest* 2012;142(4):965–72.
- Shah VP, Tunik MG, Tsung JW. Prospective evaluation of point-of-care ultrasonography for the diagnosis of pneumonia in children and young adults. *JAMA Pediatr* 2013;167(2):119–25.
- Coley BD. Chest sonography in children: current indications, techniques, and imaging findings. *Radiol Clin North Am* 2011;49(5):825–46.
- Biederer J, Beer M, Hirsch W, et al. MRI of the lung (2/3). Why ... when ... how? *Insights Imaging* 2012; 3(4):355–71.
- Montella S, Maglione M, Bruzzese D, et al. Magnetic resonance imaging is an accurate and reliable method to evaluate non-cystic fibrosis paediatric lung disease. *Respirology* 2012;17(1):87–91.
- Barreto MM, Rafful PP, Rodrigues RS, et al. Correlation between computed tomographic and magnetic resonance imaging findings of parenchymal lung diseases. *Eur J Radiol* 2013;82(9):e492–501.
- Yikilmaz A, Koc A, Coskun A, et al. Evaluation of pneumonia in children: comparison of MRI with fast imaging sequences at 1.5T with chest radiographs. *Acta Radiol* 2011;52(8):914–9.
- Gorkem SB, Coskun A, Yikilmaz A, et al. Evaluation of pediatric thoracic disorders: comparison of unenhanced fast-imaging-sequence 1.5-T MRI and contrast-enhanced MDCT. *AJR Am J Roentgenol* 2013;200(6):1352–7.
- Peprah KO, Andronikou S, Goussard P. Characteristic magnetic resonance imaging low T2 signal intensity of necrotic lung parenchyma in children

- with pulmonary tuberculosis. *J Thorac Imaging* 2012;27(3):171–4.
14. Hirsch W, Sorge I, Krohmer S, et al. MRI of the lungs in children. *Eur J Radiol* 2008;68(2):278–88.
 15. Kantarci M, Bayraktutan U, Karabulut N, et al. Alveolar echinococcosis: spectrum of findings at cross-sectional imaging. *Radiographics* 2012;32(7):2053–70.
 16. Pedrosa I, Saíz A, Arrazola J, et al. Hydatid disease: radiologic and pathologic features and complications. *Radiographics* 2000;20(3):795–817.
 17. Lee EY, Dorkin H, Vargas SO. Congenital pulmonary malformations in pediatric patients: review and update on etiology, classification, and imaging findings. *Radiol Clin North Am* 2011;49(5):921–48.
 18. Khalek N, Johnson MP. Management of prenatally diagnosed lung lesions. *Semin Pediatr Surg* 2013;22(1):24–9.
 19. Pacharn P, Kline-Fath B, Calvo-Garcia M, et al. Congenital lung lesions: prenatal MRI and postnatal findings. *Pediatr Radiol* 2013;43(9):1136–43.
 20. Recio Rodríguez M, Martínez de Vega V, Cano Alonso R, et al. MR imaging of thoracic abnormalities in the fetus. *Radiographics* 2012;32(7):E305–21.
 21. Naidich DP, Rumancik WM, Ettenger NA, et al. Congenital anomalies of the lungs in adults: MR diagnosis. *AJR Am J Roentgenol* 1988;151(1):13–9.
 22. Liszewski MC, Hersman FW, Altes TA, et al. Magnetic resonance imaging of pediatric lung parenchyma, airways, vasculature, ventilation, and perfusion: state of the art. *Radiol Clin North Am* 2013;51(4):555–82.
 23. Xu H, Jiang D, Kong X, et al. Pulmonary sequestration: three dimensional dynamic contrast-enhanced MR angiography and MRI. *J Tongji Med Univ* 2001;21(4):345–8.
 24. Peranteau WH, Merchant AM, Hedrick HL, et al. Prenatal course and postnatal management of peripheral bronchial atresia: association with congenital cystic adenomatoid malformation of the lung. *Fetal Diagn Ther* 2008;24(3):190–6.
 25. Griffin N, Devaraj A, Goldstraw P, et al. CT and histopathological correlation of congenital cystic pulmonary lesions: a common pathogenesis? *Clin Radiol* 2008;63(9):995–1005.
 26. Yu H, Li HM, Liu SY, et al. Diagnosis of arterial sequestration using multidetector CT angiography. *Eur J Radiol* 2010;76(2):274–8.
 27. Dishop MK, Kuruvilla S. Primary and metastatic lung tumors in the pediatric population: a review and 25-year experience at a large children's hospital. *Arch Pathol Lab Med* 2008;132(7):1079–103.
 28. Weldon CB, Shamberger RC. Pediatric pulmonary tumors: primary and metastatic. *Semin Pediatr Surg* 2008;17(1):17–29.
 29. Baez JC, Lee EY, Restrepo R, et al. Chest wall lesions in children. *AJR Am J Roentgenol* 2013;200(5):W402–19.
 30. Takayama Y, Yabuuchi H, Matsuo Y, et al. Computed tomographic and magnetic resonance features of inflammatory myofibroblastic tumor of the lung in children. *Radiat Med* 2008;26(10):613–7.
 31. Demir HA, Yalcin B, Ciftci AO, et al. Primary pleuropulmonary neoplasms in childhood: fourteen cases from a single center. *Asian Pac J Cancer Prev* 2011;12(2):543–7.
 32. Mut Pons R, Muro Velilla MD, Sangüesa Nebot C, et al. Pleuropulmonary blastoma in children: imaging findings and clinical patterns. *Radiologia* 2008;50(6):489–94.
 33. De Jong PA, Mayo JR, Golmohammadi K, et al. Estimation of cancer mortality associated with repetitive computed tomography scanning. *Am J Respir Crit Care Med* 2006;173(2):199–203.
 34. Chawla SC, Federman N, Zhang D, et al. Estimated cumulative radiation dose from PET/CT in children with malignancies: a 5-year retrospective review. *Pediatr Radiol* 2010;40(5):681–6.
 35. Biederer J, Hintze C, Fabel M. MRI of pulmonary nodules: technique and diagnostic value. *Cancer Imaging* 2008;8:125–30.
 36. Wu LM, Xu JR, Hua J, et al. Can diffusion-weighted imaging be used as a reliable sequence in the detection of malignant pulmonary nodules and masses? *Magn Reson Imaging* 2013;31(2):235–46.
 37. Regier M, Schwarz D, Henes FO, et al. Diffusion-weighted MR-imaging for the detection of pulmonary nodules at 1.5 Tesla: intraindividual comparison with multidetector computed tomography. *J Med Imaging Radiat Oncol* 2011;55(3):266–74.
 38. Koyama H, Ohno Y, Seki S, et al. Magnetic resonance imaging for lung cancer. *J Thorac Imaging* 2013;28(3):138–50.
 39. Lutterbey G, Gieseke J, von Falkenhausen M, et al. Lung MRI at 3.0 T: a comparison of helical CT and high-field MRI in the detection of diffuse lung disease. *Eur Radiol* 2005;15(2):324–8.
 40. Lutterbey G, Grohé C, Gieseke J, et al. Initial experience with lung-MRI at 3.0 T: comparison with CT and clinical data in the evaluation of interstitial lung disease activity. *Eur J Radiol* 2007;61(2):256–61.
 41. Müller NL, Mayo JR, Zwirewich CV. Value of MR imaging in the evaluation of chronic infiltrative lung diseases: comparison with CT. *AJR Am J Roentgenol* 1992;158(6):1205–9.
 42. Yi CA, Lee KS, Han J, et al. 3-T MRI for differentiating inflammation- and fibrosis-predominant lesions of usual and nonspecific interstitial pneumonia: comparison study with pathologic correlation. *AJR Am J Roentgenol* 2008;190(4):878–85.
 43. Eichinger M, Heussel CP, Kauczor HU, et al. Computed tomography and magnetic resonance imaging in cystic fibrosis lung disease. *J Magn Reson Imaging* 2010;32(6):1370–8.

44. Puderbach M, Hintze C, Ley S, et al. MR imaging of the chest: a practical approach at 1.5T. *Eur J Radiol* 2007;64(3):345–55.
45. Failo R, Wielopolski PA, Tiddens HA, et al. Lung morphology assessment using MRI: a robust ultra-short TR/TE 2D steady state free precession sequence used in cystic fibrosis patients. *Magn Reson Med* 2009;61(2):299–306.
46. Bauman G, Puderbach M, Heimann T, et al. Validation of Fourier decomposition MRI with dynamic contrast-enhanced MRI using visual and automated scoring of pulmonary perfusion in young cystic fibrosis patients. *Eur J Radiol* 2013;82(12):2371–7.
47. Ciet P, Wielopolski P, Manniesing R, et al. Spirometer controlled cine-magnetic resonance imaging to diagnose tracheobronchomalacia in pediatric patients. *Eur Respir J* 2014;43(1):115–24.
48. Tan JZ, Ditchfield M, Freezer N. Tracheobronchomalacia in children: review of diagnosis and definition. *Pediatr Radiol* 2012;42(8):906–15 [quiz: 1027–8].
49. Erdem E, Gokdemir Y, Unal F, et al. Flexible bronchoscopy as a valuable tool in the evaluation of infants with stridor. *Eur Arch Otorhinolaryngol* 2013;270(1):21–5.
50. Murgu S, Colt H. Tracheobronchomalacia and excessive dynamic airway collapse. *Clin Chest Med* 2013;34(3):527–55.
51. Sanchez MO, Greer MC, Masters IB, et al. A comparison of fluoroscopic airway screening with flexible bronchoscopy for diagnosing tracheomalacia. *Pediatr Pulmonol* 2012;47(1):63–7.
52. Lee EY, Strauss KJ, Tracy DA, et al. Comparison of standard-dose and reduced-dose expiratory MDCT techniques for assessment of tracheomalacia in children. *Acad Radiol* 2010;17(4):504–10.
53. Lee EY, Tracy DA, Bastos MD, et al. Expiratory volumetric MDCT evaluation of air trapping in pediatric patients with and without tracheomalacia. *AJR Am J Roentgenol* 2010;194(5):1210–5.
54. Tan JZ, Crossett M, Ditchfield M. Dynamic volumetric computed tomographic assessment of the young paediatric airway: initial experience of rapid, non-invasive, four-dimensional technique. *J Med Imaging Radiat Oncol* 2013;57(2):141–8.
55. Wagnetz U, Roberts HC, Chung T, et al. Dynamic airway evaluation with volume CT: initial experience. *Can Assoc Radiol J* 2010;61(2):90–7.
56. Wielpütz MO, Eichinger M, Puderbach M. Magnetic resonance imaging of cystic fibrosis lung disease. *J Thorac Imaging* 2013;28(3):151–9.
57. Tiddens HA, Rosenow T. What did we learn from two decades of chest computed tomography in cystic fibrosis? *Pediatr Radiol* 2014;44(12):1490–5.
58. Sileo C, Corvol H, Boelle PY, et al. HRCT and MRI of the lung in children with cystic fibrosis: comparison of different scoring systems. *J Cyst Fibros* 2014;13(2):198–204.
59. Qing K, Ruppert K, Jiang Y, et al. Regional mapping of gas uptake by blood and tissue in the human lung using hyperpolarized xenon-129 MRI. *J Magn Reson Imaging* 2014;39(2):346–59.
60. Kirby M, Parraga G. Pulmonary functional imaging using hyperpolarized noble gas MRI: six years of start-up experience at a single site. *Acad Radiol* 2013;20(11):1344–56.